

Growth of genuine multipartite entanglement in random unitary circuits

Anindita Bera¹ and Sudipto Singha Roy²

¹*Racah Institute of Physics, The Hebrew University of Jerusalem, Jerusalem 91 90401, Givat Ram, Israel*

²*Instituto de Física Teórica UAM/CSIC, C/ Nicolás Cabrera 13-15, Cantoblanco, 28049 Madrid, Spain*

(Dated: April 10, 2024)

We study the growth of genuine multipartite entanglement in random unitary circuit models consisting of both short- and long-range unitaries. We observe that circuits with short-range unitaries are optimal for generating large global entanglement, which, interestingly, is found to be close to the global entanglement in random matrix product states with moderately high bond dimension. Furthermore, the behavior of multipartite entanglement can be related to other global properties of the system, viz. the delocalization of the many-body wavefunctions. Moreover, we show that the circuit can sustain a finite amount of genuine multipartite entanglement even when it is monitored through weak measurements.

I. INTRODUCTION

Along with the studies related to quantum Hamiltonian systems, an important area that has gained much attention in recent times is the study of quantum properties related to the quantum random unitary circuits [1–13]. Even though such a model is relatively less-structured than any generic Hamiltonian system, as it only retains two fundamental features of any realistic physical systems, namely, unitarity and spatial locality, recent studies reveal that it is comprised of many rich quantum properties. It has been reported that quantum entanglement growth in these systems exhibits certain universal structure [1]. In particular, the critical exponents for the entanglement growth have been found to be similar to those of the Kardar-Parisi-Zhang (KPZ) equation, which has a wide range of applicability in non-equilibrium statistical mechanics [14]. In addition to this, both exact results and coarse-grained descriptions have been provided for the spreading of quantum operators under random quantum circuit dynamics [2, 4]. Moreover, a new class of dynamical behavior is explored, when the circuit is constantly monitored through quantum measurements [6, 8–11]. Interestingly, it has been reported that the entanglement growth of an initial product state under such random unitary dynamics, undergoes a continuous transition from the volume-law to the area-law, when it is monitored with a particular strength of the measurement [6, 8–11].

Apart from the entanglement studies, random quantum circuits have also been used to demonstrate quantum advantage through the task of sampling from the output distributions of the models [7, 12, 13]. In general, the accomplishment of such a task classically requires a direct numerical simulation of the circuit, with computational cost exponential in the number of qubits [7, 12]. Very recently, experimental validation of the same has also been reported in Ref. [13]. All this progress has significantly increased the interest of the community to explore several other quantum properties related to random circuit models.

To date, among the works related to random unitary circuit models, the study of local or bipartite quantum properties has received most of the attention. The be-

havior of global properties in these models remains an interesting area to explore. Multipartite entanglement is one such important property which is also considered to be a potential resource in many quantum information and computation protocols [15–20]. In recent years, several studies endorse the fact that along with bipartite entanglement, multipartite entanglement can also faithfully detect quantum phase transitions in several quantum many-body systems [21–27]. Moreover, using recent technologies, experimental realizations and manipulation of multipartite entangled states have also been reported in atomic, ion-trap and optical settings [28–33].

In this work, we aim at studying the global properties of random unitary circuits. In particular, we look at the multipartite entanglement properties of the quantum state obtained at each iteration of a random unitary circuit and relate it to other physical properties of the system. We observe that an initial product state when subjected to a random unitary circuit, acquires a substantial amount of genuine multipartite entanglement even for a few iterations of the circuit, and at large iteration time, eventually saturates to a very high value, close to the maximum possible value in qubit systems. Additionally, we find that the saturated value of genuine multipartite entanglement has very little dependence on the range of interactions. For instance, at large iteration time, random unitary circuit models comprised of quasi-long-range and long-range unitaries provide almost the same amount of multipartite entanglement as that obtained for the short-range case. However, the growth rate of multipartite entanglement varies depending on the range of unitaries. We then compare the behavior of multipartite entanglement obtained for the random unitary circuit to that obtained for the random matrix product states (RMPS). This provides us a framework to characterize the complexity of the random state generated at a large time in terms of the bond dimension of the random matrix product states. In particular, we observe that random matrix product states with a bond dimension that grows polynomially with the system size, can attain multipartite entanglement close to the value obtained for the random quantum state generated at a large time in the random unitary circuit models.

Once the multipartite entanglement properties of the circuits are fully characterized, we next relate that to other global properties of these models. In particular, we study the delocalization of the initial wavefunction when it is subjected to the quantum dynamics under the random unitary circuits. In general, for any generic quantum many-body wavefunction, the relation between its spread in the Hilbert space or delocalization and its global entanglement content is not obvious [34–36]. For instance, there are highly localized quantum states which can exhibit a high amount of genuine multipartite entanglement, e.g. the GHZ state. On the other hand, though the entanglement content of both the states $|0\rangle^{\otimes N}$ and $|+\rangle^{\otimes N}$ is zero and the former one is completely localized, the latter has uniform spread over all the points in the Hilbert space. In the case of a Hamiltonian system, it has been extensively studied that the presence of randomness in the static field often leads to localization of quantum many-body wavefunctions and leaves those as nearly product states [37–44]. Therefore, it is an interesting case to investigate how it affects the localization properties of the highly entangled random many-body wavefunction obtained at each iteration step of the circuit. In this regard, we compute the inverse-participation-ratio (IPR), a commonly used measure of localization of the wavefunctions, and observe that the qualitative behavior of these two global properties of the circuit is very close to each other. Like the global entanglement, IPR grows rapidly and then eventually saturates at a high value, which indicates fast delocalization of the initial wavefunctions. Therefore, we can argue that in the random unitary circuit models, the spreading of the quantum many-body wavefunctions in Hilbert space and the growth of multipartite entanglement have close correspondence.

Finally, we analyze the robustness of multipartite entanglement of the random quantum state generated for a large number of circuit iterations, when it is monitored through non-projective or unsharp or weak measurements [45–47], which are a special subset of positive-operator-valued-measurements (POVMs). We report that the random quantum state sustains a non-zero amount of global entanglement, even for high values of the measurement strength. Interestingly, the decay pattern of global entanglement with the measurement strength becomes almost similar to that obtained for an N -qubit GHZ state. Therefore, we argue that random unitary circuits, even though result in a less-structured quantum dynamics than a generic Hamiltonian system, generate a high amount of global entanglement, which remains non-zero under monitoring through weak measurements and thus can serve as a potential resource in quantum information and computation tasks which are accomplished exploiting multipartite entanglement.

We arrange the paper in the following way. In Sec. II, we describe the random unitary circuit that we consider in our work. In Sec. III, we briefly discuss the measure of genuine multipartite entanglement. Next, in Sec. IV, we demonstrate the growth of genuine multipartite entangle-

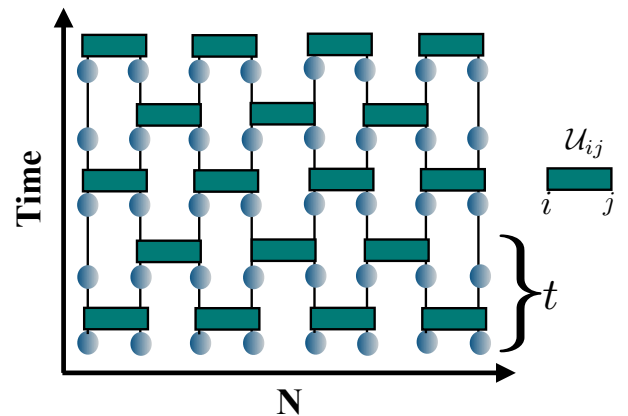


FIG. 1. Schematic representation of the random unitary circuit. The solid circles indicate the lattice sites and the rectangular boxes represent the random unitaries U_{ij} acting on sites i and j . The abscissa and ordinate correspond to the number of sites N of the circuit and the evolution time respectively. A complete iteration is denoted by t .

ment with each iteration step of the circuit and compare it with that obtained for some other possible variants of the circuits. In Sec. V, we compare the behavior of multipartite entanglement obtained for the random state generated at a large iteration of the random unitary circuit to that obtained for a random matrix product state. A comparison between two global properties of the circuit, namely, the spread of wavefunctions in Hilbert space and the multipartite entanglement are made in Sec. VI. Next, in Sec. VII, we discuss the robustness of the multipartite entanglement generated in the random unitary circuit under the effect of weak measurements. Finally, we conclude in Sec. VIII.

II. THE MODEL

Let us briefly discuss the random unitary circuit as depicted in Fig. 1. In this circuit, we first apply random unitaries U_{ij} , generated independently through Haar measure, on the nearest neighbor sites (i, j) i.e. on the sites $(1, 2), (3, 4), (5, 6), \dots, (N-1, N)$, where N is the total number of sites. In the next step, we apply the unitaries on the remaining nearest-neighbor pairs of sites, i.e., $(2, 3), (4, 5), (6, 7), \dots, (N-2, N-1)$. This completes a full iteration, denoted by t . The number of unitaries acting at each iteration is $N-1$. As the interactions between spins or qubits are taken to be random in both space and time, it becomes a less-structured model than any generic Hamiltonian system. Note here that throughout the paper, we mainly consider the random states generated through the short-range random unitary circuits discussed above. However, in our work we also study some of the variants of random unitary circuits, which we discuss in detail in Sec. IV.

III. GENUINE MULTIPARTITE ENTANGLEMENT AND ITS MEASURE

In this section, we briefly introduce the measure of genuine multipartite entanglement that we consider in our work. An N -party pure quantum state is said to be genuinely multipartite entangled if it cannot be written as a product in any possible bipartitions of the state [48–52]. An example of such quantum state is the N -party GHZ state, given by $|\psi\rangle_{\text{GHZ}} = \frac{1}{\sqrt{2}}(|0\rangle^{\otimes N} + |1\rangle^{\otimes N})$. In order to quantify the genuine multipartite entanglement of any pure quantum state $|\Psi\rangle_N$, we consider a computable measure known as the generalized geometric measure (GGM) [50–52]. It is defined as an optimized distance of the given quantum state, $|\Psi\rangle_N$, from the set of all states that are not genuinely multipartite entangled. This can be mathematically expressed as

$$\mathcal{G}(|\Psi\rangle_N) = 1 - \zeta_{\max}^2(|\Psi\rangle_N), \quad (1)$$

where $\zeta_{\max}(|\Psi\rangle_N) = \max |\langle \eta | \Psi \rangle_N|$, with the maximization being carried out over all pure N -party quantum state $|\eta\rangle$ which are not genuinely multipartite entangled. Further simplification of the above equation leads to an equivalent expression, given by

$$\mathcal{G}(|\Psi\rangle_N) = 1 - \max\{\lambda_{A:B} | A \cup B = \{1, 2, \dots, N\}, A \cap B = \emptyset\}, \quad (2)$$

where $\lambda_{A:B}$ is the largest eigenvalue of the reduced density matrix ρ_A or ρ_B of $|\Psi\rangle_N$. For the qubit system, the value of \mathcal{G} lies within the range $0 \leq \mathcal{G} \leq 0.5$.

IV. GROWTH OF MULTIPARTITE ENTANGLEMENT

We are now equipped with the necessary tools to study the global entanglement properties of an initial product state when it is iteratively subjected to the random quantum circuit described in Fig. 1. Towards this aim, we start with the initial product state $|\Psi(t=0)\rangle = |0\rangle^{\otimes N}$ and compute its GGM (\mathcal{G}) at each step of the iteration of the circuit. The number of random realizations of the circuit considered here is 10^2 . The behavior of the multipartite entanglement averaged over all such random realizations of the circuit with the iteration number t is depicted in Fig. 2. From the figure, we note that \mathcal{G} grows very fast and saturates eventually to a high value for large iteration times. We denote the saturation value of multipartite entanglement by \mathcal{G}_{sat} , which is the value of \mathcal{G} , obtained after 20 iterations of the circuit, i.e., $\mathcal{G}_{\text{sat}} = \mathcal{G}(|\psi(t=20)\rangle)$. For $N = 12$, $\mathcal{G}_{\text{sat}} = 0.478$. Subsequently, in order to find an analytical form of $\mathcal{G}(t)$ (see the inset (a) of Fig. 2), we fit $\mathcal{G}/\mathcal{G}_{\text{sat}}$ and find that \mathcal{G} grows approximately as

$$\mathcal{G}(t) = \mathcal{G}_{\text{sat}} \tanh\left(\frac{t}{t_0}\right), \quad (3)$$

with $t_0 \approx 6$. A scaling analysis of \mathcal{G} with N is also presented in the inset (b) which indicates that even for

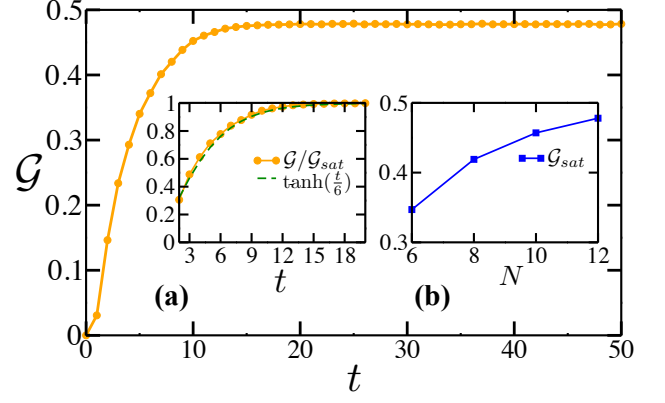


FIG. 2. The growth of \mathcal{G} with iteration number t . At each iteration, the averaging of \mathcal{G} is performed over 10^2 random realizations of the unitaries. Here $N = 12$. Inset (a) shows the fitting of $\mathcal{G}/\mathcal{G}_{\text{sat}}$ vs. t profile which is close to the function $\tanh(\frac{t}{6})$. Inset (b) exhibits the scaling of \mathcal{G}_{sat} with N .

moderate system-size, $N = 12$, the multipartite entanglement content of the random state at high iteration number eventually becomes very close to the maximum value of global entanglement in qubit systems.

In addition to this, we observe that the circuit configuration in Fig. 1 is the optimal one, in the sense that if we consider other variants of the circuit, where instead of short-range unitaries, the circuit comprises of unitaries acting on non-nearest neighbor qubits, there is no advantage of the multipartite entanglement generated at high iteration. We show a schematic representation of all such configurations in Fig. 3.

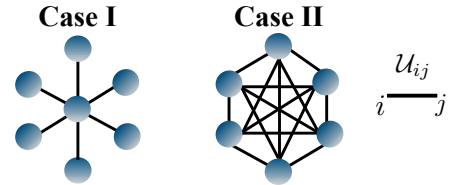


FIG. 3. Schematic representation of different configurations of random unitary circuits. Case I illustrates the quasi long-range circuit where one qubit is connected with the rest of the $N - 1$ qubits. Case II depicts a complete long-range circuit where each of the qubits is connected with all the other qubits. The solid black line represents the unitary \mathcal{U}_{ij} acting on the qubits i and j at its two edges.

In Case I, we consider a quasi long-range unitary circuit, such that two-qubit unitaries are now acting on the first qubit and rest of the qubits, i.e., $\Pi_{r=2}^N \mathcal{U}_{1r}$. Here, the number of unitaries remains the same as the previous case, which is $N - 1$. Case II demonstrates a proper long-range scenario in the sense that all the N qubits are now connected with each other through the two-qubit unitaries, $\Pi_{i < j, i, j=1}^N \mathcal{U}_{ij}$. The number of unitaries acting in the circuit at each iteration step is given

by $\frac{N}{2}(N-1)$. We observe that similar to the short-range random unitary circuit, multipartite entanglement in quasi long-range and long-range circuits grow fast with the iteration steps and the final value to which it saturates is very close to that obtained for the short-range case. Hence, long-range interaction does not provide much benefit in terms of the saturation value of multipartite entanglement. However, from our analysis, we note that the growth rate has a dependence on the range of unitaries. A comparison of such different growth rates can be made from the fitted values of the multipartite entanglement. The growth of multipartite entanglement in these cases can again be approximated using Eq. (3), which yields

$$\begin{aligned} \text{Case I : } t_0 &\approx 4, \\ \text{Case II : } t_0 &\approx 1. \end{aligned} \quad (4)$$

Therefore, though at an initial time, multipartite entanglement obtained in these cases could slightly differ from each other, and saturation may begin at different values of t , the final value to which it ultimately saturates is almost the same for all the cases.

This essentially completes the first part of our analysis. In the forthcoming sections, we study several other relevant physical quantities and provide a detailed characterization of the random quantum state generated through such random unitary dynamics.

V. COMPARISON TO RANDOM MATRIX PRODUCT STATES

We now compare the growth of multipartite entanglement obtained for random unitary circuit models as discussed in the previous section, to that obtained for random matrix product states. Matrix product states (MPS) with fixed bond dimension lie in a tiny corner of the total Hilbert space and are often found to be an approximate ground state of local Hamiltonians [53–55]. As stated earlier, the random unitary circuit models represent a less-structured model than the Hamiltonian systems, and the presence of randomness eventually pushes the quantum state to occupy a wider region within the Hilbert space. Therefore, the behavior of multipartite entanglement in random MPS and its comparison with the random quantum state generated through the random unitary circuit model is an interesting case to explore. In Ref. [56], it has been reported that a set of non-homogeneous random MPS and the set of uniformly distributed general random states yield the same average states. Here, our aim is to explore whether any such similarity exists between these two differently constructed random states when the multipartite entanglement properties are considered.

We start with the matrix product states representation of any pure quantum state $|\Psi\rangle$, which is given by

$$|\Psi\rangle = \sum_{i_1 i_2 \dots i_N} \text{Tr}(A_1^{i_1} A_2^{i_2} \dots A_N^{i_N}) |i_1 i_2 \dots i_N\rangle, \quad (5)$$

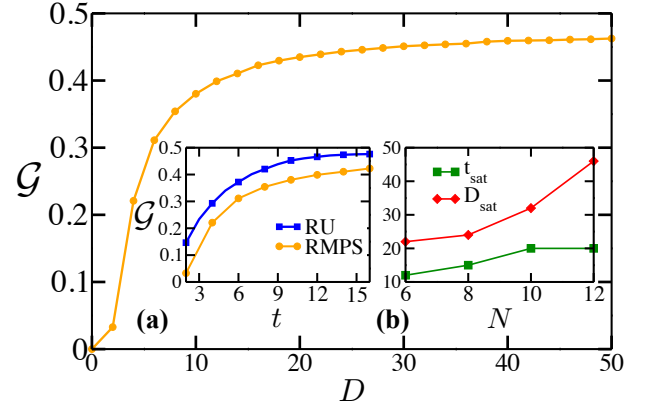


FIG. 4. Growth of \mathcal{G} in RMPS with the bond dimension D . Here, $N = 12$ and the averaging of \mathcal{G} is performed over 10^2 random realizations. In the inset (a), a comparison between the growth of \mathcal{G} in random unitary circuit (RU) (blue curve) and random matrix product states (RMPS) (orange curve) for a small time $t (= D)$ is presented. The inset (b) depicts the scaling of the saturated iteration number (t_{sat}) and saturated bond dimension (D_{sat}) for random unitary circuit and random MPS, respectively, with the system size N .

where $A_k^{i_k}$ are $D \times D$ complex matrices, with D being the bond dimension. In general, in order to represent any quantum state in MPS form, one requires ND^2d number of parameters, where d is the local Hilbert space dimension of the system (for qubits $d = 2$). For small D , this number turns out to be much smaller than the dimension of the actual Hilbert space, d^N .

In this work, we consider a matrix product state, where the $A_k^{i_k}$ matrices are random unitaries \mathcal{U} of dimensions $D \times D$ and aim to find the growth of genuine multipartite entanglement with its bond dimension D . Fig. 4 shows the growth of \mathcal{G} of a RMPS with D . For each D , averaging of \mathcal{G} is performed over 10^2 random realizations of the matrix product states. We find that for small values of D , the value of GGM obtained for RMPS turns out to be lower than that obtained for the random quantum state generated after $t = D$ times iteration of the random unitary circuit (see the inset (a) of Fig. 4). However, with increasing bond dimension, multipartite entanglement in RMPS increases and finally saturates at a value $\mathcal{G} = 0.463$, which is very close to that obtained for the random circuit. Hence, we can argue that in terms of global entanglement content, the random quantum state generated at high iteration time of the circuit is comparable to a random MPS with a moderately large bond dimension.

In addition to this, the inset (b) of Fig. 4 depicts a comparison between the scalings of the iteration number (t_{sat}) in the random unitary circuit and the bond dimension (D_{sat}) in RMPS when \mathcal{G} saturates in both the systems. We note that in the random circuit model, t_{sat} initially increases with N and eventually saturates, even for moderately large system size. On the contrary,

D_{sat} in random MPS does not show any such tendency, and continues to grow polynomially with the system size ($D_{sat}(N) \approx aN^2 + bN + c$, with a, b, c constants). This suggests, for large N , in order to have multipartite entanglement close to the saturated value obtained in random unitary circuit models, one needs to consider RMPS with a bond dimension which is polynomial in the system size. Nevertheless, efficient generation of such random matrix product states still remains a relatively easier task than the exact preparation of random unitary circuits with a large number of qubits.

VI. DELOCALIZATION OF THE WAVEFUNCTION

Along with the studies of the multipartite entanglement properties of the random unitary circuits, we also study other global property of the models, namely, the delocalization of an initial product state, when it evolves under the interactions of the random unitaries. Importantly, this gives us an opportunity to compare the spread of wavefunctions in Hilbert space with the spread of entanglement in different bipartitions of a multipartite quantum state. In order to quantify the degree of delocalization of any quantum state in Hilbert space, we consider a commonly used measure, known as the Inverse Participation Ratio (IPR) [43]. It can be expressed as

$$\text{IPR} = \frac{1}{\sum_{i=1}^{2^N} |\langle \Psi(t) | i \rangle|^4}, \quad (6)$$

where $\{|i\rangle\}_{i=1}^{2^N}$ is the computational basis. In general, for a completely delocalized state, one gets $\langle i | \Psi(t) \rangle = \frac{1}{\sqrt{2^N}}$, $\forall i$, implying that $\text{IPR} = 2^N$. On the other hand, for a completely localized state, we have $\text{IPR} = 1$. In both limits, multipartite entanglement becomes zero. However, there could be other states e.g., $|\psi\rangle_{\text{GHZ}}$, for which IPR is very low but the multipartite entanglement content is maximum, i.e. $\mathcal{G} = 0.5$. Therefore, for any generic quantum system, the exact relation between delocalization of the wavefunctions and its multipartite entanglement content is not obvious. In this regard, the relation between IPR and bipartite entanglement, quantified by entanglement entropy, is discussed for a set of random states drawn from various ensembles [34, 35] and also for the eigenstates of certain local many-body Hamiltonians [36].

To investigate the relation between delocalization and growth of multipartite entanglement in the quantum random unitary circuit, we start with the same initial state $|\Psi(t=0)\rangle = |0\rangle^{\otimes N}$ and compute its IPR at each iteration of the circuit. Fig. 5 illustrates the growth of IPR with the iteration number t . Like all other quantities we have previously computed, IPR is averaged over 10^2 random realizations of the circuit. We observe that the IPR increases very fast and eventually saturates at a high value. Clearly, this behavior is qualitatively similar to that of \mathcal{G} ,

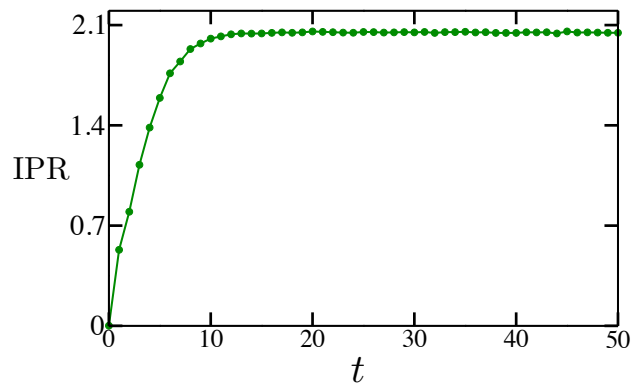


FIG. 5. The growth of IPR with the iteration number t . Here, y axis has been rescaled by a factor, $y = y \times 10^{-3}$. The number of random unitary realizations for each iteration is 10^2 and $N = 12$.

depicted in Fig. 2 and remains very much distinct from the localization property of GHZ state. Therefore, from the comparison, we argue that for the random unitary circuit we consider in our work, the spreading of wavefunctions in Hilbert space and the growth of multipartite entanglement present a close correspondence.

We have now fully characterized the properties of the random quantum state generated through the dynamics of the random unitary circuits. However, along with the generation of such highly entangled random quantum states, to use it as a resource for quantum information processing and computational tasks, it is equally important to investigate its robustness properties. In the next section, we consider one such set-up and discuss its robustness properties in detail.

VII. ROBUSTNESS OF MULTIPARTITE ENTANGLEMENT

Apart from its fundamental importance, quantum measurements have a wide range of applications in various measurement-based quantum information processing and computation tasks, viz. quantum state manipulation [57–59], entanglement protection [60, 61], measurement-based quantum computation [17, 62], etc. In the case of measurement-based quantum information and computation schemes, starting from a highly entangled resource state, sequential measurements are applied to exploit the shared entanglement in accomplishing the desired tasks. In this way, the initial resource is irreversibly degraded as the computation proceeds and reusability of the resource ceases. One way to minimize the effects of such quantum measurements is to apply the weak measurement schemes [45–47, 63, 64]. Though this, in turn, may affect the efficiency of the protocol, the reusability of the resource opens up. In the case of the genuine multipartite entangled state, quantum measurement has an adverse effect on its multipartite entangle-

ment content. Here, even a single qubit measurement is sufficient to transform it into a completely product state in some bipartition. Hence, for reusability of the genuine multipartite entangled state in measurement-based quantum information processing and computational tasks, weak measurement schemes are a potential choice. This motivates us to investigate how robust the multipartite entanglement generated in the random unitary circuits is under the effect of weak measurements.

Towards this aim, we consider weak measurement operators, $M_{\pm}^{\lambda} = \frac{I \pm \lambda \sigma_z}{\sqrt{2(1+\lambda^2)}}$, characterized by the parameter $0 < \lambda \leq 1$. These measurement operators satisfy the completeness relation: $M_{+}^{\lambda} M_{+}^{\lambda\dagger} + M_{-}^{\lambda} M_{-}^{\lambda\dagger} = \mathbb{I}$. The parameter λ represents the measurement strength. Indeed, for $\lambda = 1$, M_{\pm}^{λ} correspond to projective measurements. We perform M_{\pm}^{λ} on the quantum state generated at large iteration time of the random unitary circuit and the position of such measurements is completely random. For a schematic depiction, see Fig. 6(a). The quantum state after performing the weak measurement is then reads as $|\Psi(t)\rangle_{\pm}^{\lambda} = \frac{M_{\pm}^{\lambda} |\Psi(t)\rangle}{\|M_{\pm}^{\lambda} |\Psi(t)\rangle\|}$. The procedure is repeated for a large number of measurements (10^2) and the final value of the global entanglement is obtained by averaging over all such outcomes and a large number of random realizations of the circuits (10^2). The behavior of the saturated value of global entanglement, denoted by $\mathcal{G}_{sat}^{\lambda}$, with the measurement strength λ is depicted in Fig. 6(b). From the figure, we find that the multipartite entanglement of the random state obtained at high iteration time exhibits a polynomial decay with the strength of measurement, which can be analytically expressed as

$$\mathcal{G}_{Sat}^{\lambda} \approx \frac{(1-\lambda)^2}{2(1+\lambda^2)}. \quad (7)$$

Interestingly, the above analytical form coincides exactly with the decay profile of multipartite entanglement of an N -qubit pure GHZ state.

Therefore, we observe that though the quantum state generated for a large number of circuit iteration remains highly delocalized, the value of its global entanglement and decay pattern under weak measurements remain akin to that of N -qubit GHZ state.

VIII. CONCLUSION

In this work, we analyzed the global properties of the random unitary circuits, which are generally considered as least-structured models for quantum dynamics. We considered random unitary circuits comprised of short-range, quasi-long-range, and fully long-range unitaries and studied the growth of genuine multipartite entanglement when an initial product state is iteratively subjected to those circuits. We observed that the initial product state accumulates a high amount of multipartite entanglement even after a few iterations of the circuits.

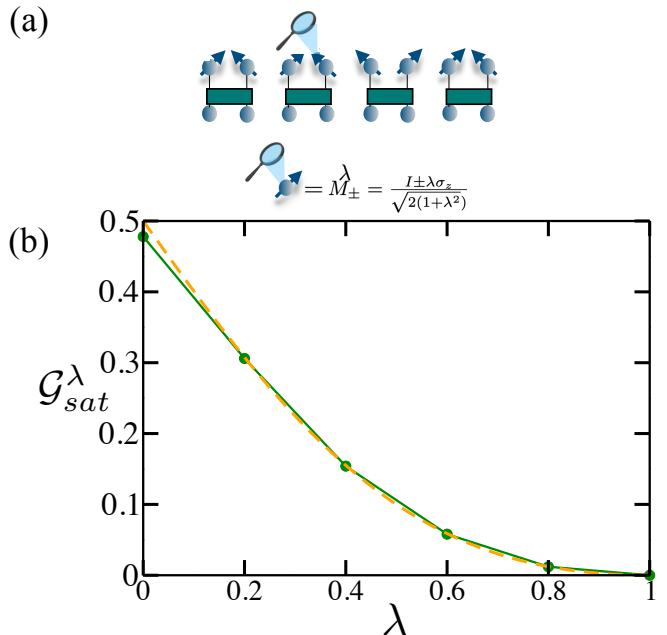


FIG. 6. Depiction of weak measurement settings. Panel (a) represents a schematic sketch of the weak measurements M_{\pm}^{λ} performed on any qubit randomly chosen from the N sites. Panel (b) displays the decreasing behavior of saturation value of multipartite entanglement $\mathcal{G}_{sat}^{\lambda}$ with measurement strength λ . The dashed orange line signifies the fitted analytical expression given in Eq. (7). Here, $N = 12$ and the number of random realizations of the circuit is 10^2 .

Moreover, the saturated value of global entanglement obtained for moderately large iteration time has very little dependence on the range of unitaries and generates almost the same amount of global entanglement even if the range or the number of unitaries are increased. We then compared the behavior of global entanglement obtained for this circuit to that of the random matrix product states. We report that the behavior of genuine multipartite entanglement is very similar in both cases. In particular, we observed that a random matrix product state with a bond dimension which is polynomial in system size, can attain the value of genuine multipartite entanglement close to that obtained for the random state generated for large iteration of the random unitary circuits. In addition to this, we made a connection between the behavior of multipartite entanglement with the other global properties of the system, such as the delocalization of the initial wavefunctions and observed a very close correspondence between these two global quantities. Finally, we studied the robustness of the multipartite entanglement generated through such random unitary dynamics, under the effect of weak measurements performed on any qubit, randomly chosen from N sites. We showed that the circuit sustains a non-zero amount of global entanglement even when the strength of the measurement is very high.

ACKNOWLEDGEMENTS

The Authors thank H. S. Dhar, U. Sen, J. Rodríguez Laguna and G. Sierra for providing their fruitful suggestions. SSR acknowledges Ministerio de Ciencia,

Innovacin y Universidades (grant PGC2018-095862-B-C21), the Comunidad de Madrid (grant QUITEMAD+S2013/ICE-2801), the Centro de Excelencia Severo Ochoa Programme (grant SEV-2016-0597) and the CSIC Research Platform on Quantum Technologies PTI-001.

-
- [1] A. Nahum, J. Ruhman, S. Vijay, and J. Haah, *Quantum Entanglement Growth under Random Unitary Dynamics*, Phys. Rev. X **7**, 031016 (2017).
 - [2] A. Nahum, S. Vijay, and J. Haah, *Operator Spreading in Random Unitary Circuits*, Phys. Rev. X **8**, 021014 (2018).
 - [3] V. Khemani, A. Vishwanath, and D. A. Huse, *Operator Spreading and the Emergence of Dissipative Hydrodynamics under Unitary Evolution with Conservation Laws*, Phys. Rev. X **8**, 031057 (2018).
 - [4] C. W. von Keyserlingk, T. Rakovszky, F. Pollmann, and S. L. Sondhi, *Operator Hydrodynamics, OTOCs, and Entanglement Growth in Systems without Conservation Laws*, Phys. Rev. X **8**, 021013 (2018).
 - [5] A. Chan, A. De Luca, and J. T. Chalker, *Solution of a Minimal Model for Many-Body Quantum Chaos*, Phys. Rev. X **8**, 041019 (2018).
 - [6] Y. Li, X. Chen, and M. P. A. Fisher, *Quantum Zeno effect and the many-body entanglement transition*, Phys. Rev. B **98**, 205136 (2018).
 - [7] S. Boixo, S. V. Isakov, V. N. Smelyanskiy, R. Babbush, N. Ding, Z. Jiang, M. J. Bremner, J. M. Martinis, and H. Neven, *Characterizing Quantum Supremacy in Near-Term Devices*, Nat. Phys **14**, 595 (2018).
 - [8] B. Skinner, J. Ruhman, and A. Nahum, *Measurement-Induced Phase Transitions in the Dynamics of Entanglement*, Phys. Rev. X **9**, 031009 (2019).
 - [9] M. Szyniszewski, A. Romito, and H. Schomerus, *Entanglement transition from variable-strength weak measurements*, Phys. Rev. B **100**, 064204 (2019).
 - [10] T. Zhou and A. Nahum, *Emergent statistical mechanics of entanglement in random unitary circuits*, Phys. Rev. B **99**, 174205 (2019).
 - [11] A. Chan, R. M. Nandkishore, M. Pretko, and G. Smith, *Unitary-projective entanglement dynamics*, Phys. Rev. B **99**, 224307 (2019).
 - [12] A. Bouland, B. Fefferman, C. Nirkhe, and U. Vazirani, *On the complexity and verification of quantum random circuit sampling*, Nat. Phys **15**, 159 (2019).
 - [13] F. Arute, K. Arya, R. Babbush, D. Bacon, J. C. Bardin, R. Barends, R. Biswas, S. Boixo, F. G. S. L. Brandao, D. A. Buell, et al., *Quantum supremacy using a programmable superconducting processor*, Nature **574**, 505 (2019).
 - [14] M. Kardar, G. Parisi, and Y-C. Zhang, *Dynamic scaling of growing interfaces*, Phys. Rev. Lett. **56**, 889 (1986).
 - [15] A. Karlsson and M. Bourennane, *Quantum teleportation using three-particle entanglement*, Phys. Rev. A **58**, 4394 (1998).
 - [16] S. Bandyopadhyay, *Teleportation and secret sharing with pure entangled states*, Phys. Rev. A **62**, 012308 (2000).
 - [17] R. Raussendorf and H. J. Briegel, *A one-way quantum computer*, Phys. Rev. Lett. **86**, 5188 (2001).
 - [18] G. Rigolin, *Quantum teleportation of an arbitrary two-qubit state and its relation to multipartite entanglement*, Phys. Rev. A **71**, 032303 (2005).
 - [19] Y. Yeo and W. K. Chua, *Teleportation and Dense Coding with Genuine Multipartite Entanglement*, Phys. Rev. Lett. **96**, 060502 (2006).
 - [20] P. Agrawal and A. Pati, *Perfect teleportation and superdense coding with W-states*, Phys. Rev. A **74**, 062320 (2006).
 - [21] T.-C. Wei, D. Das, S. Mukhopadhyay, S. Vishveshwara, and P. M. Goldbart, *Global entanglement and quantum criticality in spin chains*, Phys. Rev. A **71**, 060305(R) (2005).
 - [22] H. T. Cui, *Multiparticle entanglement in the Lipkin-Meshkov-Glick model*, Phys. Rev. A **77**, 052105 (2008).
 - [23] R. Orús, *Universal Geometric Entanglement Close to Quantum Phase Transitions*, Phys. Rev. Lett. **100**, 130502 (2008).
 - [24] S. M. Giampaolo and B. C. Hiesmayr, *Genuine multipartite entanglement in the XY model*, Phys. Rev. A **88**, 052305 (2013).
 - [25] J. Stasinska, B. Rogers, M. Paternostro, G. De Chiara, and A. Sanpera, *Long-range multipartite entanglement close to a first-order quantum phase transition*, Phys. Rev. A **89**, 032330 (2014).
 - [26] M. Hofmann, A. Osterloh, and O. Gühne, *Scaling of genuine multiparticle entanglement close to a quantum phase transition*, Phys. Rev. B **89**, 134101 (2014).
 - [27] S. S. Roy, H. S. Dhar, D. Rakshit, A. Sen(De), and U. Sen, *Detecting phase boundaries of quantum spin-1/2 XXZ ladder via bipartite and multipartite entanglement transitions*, J. Magn. Magn. Mater. **444**, 227 (2017).
 - [28] M. Eibl, N. Kiesel, M. Bourennane, C. Kurtsiefer, and H. Weinfurter, *Experimental Realization of a Three-Qubit Entangled W State*, Phys. Rev. Lett. **92**, 077901 (2004).
 - [29] N. Kiesel, C. Schmid, G. Tóth, E. Solano, and H. Weinfurter, *Experimental Observation of Four-Photon Entangled Dicke State with High Fidelity*, Phys. Rev. Lett. **98**, 063604 (2007).
 - [30] R. Prevedel, G. Cronenberg, M. S. Tame, M. Paternostro, P. Walther, M. S. Kim, and A. Zeilinger, *Experimental Realization of Dicke States of up to Six Qubits for Multiparty Quantum Networking*, Phys. Rev. Lett. **103**, 020503 (2009).
 - [31] W. B. Gao, C. Y. Lu, X. C. Yao, P. Xu, O. Gühne, A. Goebel, Y. A. Chen, C. Z. Peng, Z. B. Chen, and J. W. Pan, *Experimental demonstration of a hyperentangled ten-qubit Schrödinger cat state*, Nat. Phys. **6**, 331 (2010).
 - [32] J. W. Pan, Z. B. Chen, C. Y. Lu, H. Weinfurter, A. Zeilinger, and M. Żukowski, *Multiphoton entanglement and interferometry*, Rev. Mod. Phys. **84**, 777 (2012).
 - [33] X. C. Yao, T. X. Wang, P. Xu, H. Lu, G. S. Pan, X. H. Bao, C. Z. Peng, C. Y. Lu, Y. A. Chen, and J. W. Pan, *Observation of eight-photon entanglement*, Nat. Photonics **6**, 225 (2012).

- [34] O. Giraud, J. Martin, and B. Georgeot, *Entanglement of localized states*, Phys. Rev. A **76**, 042333 (2007).
- [35] O. Giraud, J. Martin, and B. Georgeot, *Entropy of entanglement and multifractal exponents for random states*, Phys. Rev. A **79**, 032308 (2009).
- [36] W. Beugeling, A. Andreanov, and M. Haque, *Global characteristics of all eigenstates of local many-body Hamiltonians: participation ratio and entanglement entropy*, J. Stat. Mech. **P02002** (2015).
- [37] M. Žnidarič, T. Prosen, and P. Prelovsek, *Many-body localization in the Heisenberg XXZ magnet in a random field*, Phys. Rev. B **77**, 064426 (2008).
- [38] V. Oganesyan, A. Pal, and D. A. Huse, *Energy transport in disordered classical spin chains*, Phys. Rev. B **80**, 115104 (2009).
- [39] A. Pal and D. A. Huse, *Many-body localization phase transition*, Phys. Rev. B **82**, 174411 (2010).
- [40] M. Schreiber, S. S. Hodgman, P. Bordia, H. P. Lüschen, M. H. Fischer, R. Vosk, E. Altman, U. Schneider, and I. Bloch, *Observation of many-body localization of interacting fermions in a quasi-random optical lattice*, Science **349**, 842 (2015).
- [41] J. Smith, A. Lee, P. Richerme, B. Neyenhuis, P. W. Hess, P. Hauke, M. Heyl, D. A. Huse, and C. Monroe, *Many-body localization in a quantum simulator with programmable random disorder*, Nat. Phys. **12**, 907 (2016).
- [42] D. A. Abanin and Z. Papić, *Recent progress in many-body localization*, Ann. Phys. (Berlin) **529**, 1700169 (2017).
- [43] F. Alet and N. Laflorencie, *Many-body localization: An introduction and selected topics*, C. R. Phys. **19**, 498 (2018), and references therein.
- [44] S. Singha Roy, U. Mishra, and D. Rakshit, *Trends of information backflow in disordered spin chains*, Euro Phys. Lett. **129** 30005 (2020).
- [45] Y. Aharonov, P. G. Bergmann, and J. L. Lebowitz, *Time Symmetry in the Quantum Process of Measurement*, Phys. Rev. **134**, B1410 (1964).
- [46] P. Busch, *Unsharp reality and joint measurements for spin observables*, Phys. Rev. D **33**, 2253 (1986).
- [47] P. Busch, P. J. Lahti, and P. Mittelstaedt, *The Quantum Theory of Measurement*, Springer: Berlin, Germany, 1996.
- [48] T. C. Wei and P. M. Goldbart, *Geometric measure of entanglement and applications to bipartite and multipartite quantum states*, Phys. Rev. A **68**, 042307 (2003).
- [49] M. Blasone, F. Dell'Anno, S. DeSiena, and F. Illuminati, *Hierarchies of geometric entanglement*, Phys. Rev. A **77**, 062304 (2008).
- [50] A. Sen(De) and U. Sen, *Channel capacities versus entanglement measures in multiparty quantum states*, Phys. Rev. A **81**, 012308 (2010).
- [51] A. Sen(De) and U. Sen, *Bound Genuine Multisite Entanglement: Detector of Gapless-Gapped Quantum Transitions in Frustrated Systems*, arXiv:1002.1253 [quant-ph].
- [52] G. D. Chiara and A. Sanpera, *Genuine quantum correlations in quantum many-body systems: a review of recent progress*, Rep. Prog. Phys. **81**, 074002 (2018).
- [53] F. Verstraete, J. I. Cirac, and V. Murg, *Matrix product states, projected entangled pair states, and variational renormalization group methods for quantum spin systems*, Adv. Phys. **57**, 143 (2008).
- [54] J. I. Cirac and F. Verstraete, *Renormalization and tensor product states in spin chains and lattices*, J. Phys. A **42**, 504004 (2009).
- [55] R. Orús, *A Practical Introduction to Tensor Networks: Matrix Product States and Projected Entangled Pair States*, Ann. Phys. **349**, 117 (2014).
- [56] S. Garnerone, T. R. de Oliveira, S. Haas, and P. Zanardi, *Statistical properties of random matrix product states*, Phys. Rev. A **82**, 052312 (2010).
- [57] S. Ashhab and F. Nori, *Control-free control: Manipulating a quantum system using only a limited set of measurements*, Phys. Rev. A **82**, 062103 (2010).
- [58] M. S. Blok, C. Bonato, M. L. Markham, D. J. Twitchen, V. V. Dobrovitski, and R. Hanson, *Manipulating a qubit through the backaction of sequential partial measurements and real-time feedback*, Nat. Phys. **10**, 189 (2014).
- [59] S. Fu, G. Shi, A. Proutiere, and M. R. James, *Feedback policies for measurement-based quantum state manipulation*, Phys. Rev. A **90**, 062328 (2014).
- [60] Y. S. Kim, J. C. Lee, O. Kwon, and Y. H. Kim, *Protecting entanglement from decoherence using weak measurement and quantum measurement reversal*, Nat. Phys. **8**, 1117 (2012).
- [61] C. Huang, W. Ma, and L. Ye, *Protecting quantum entanglement and correlation by local filtering operations*, Quant. Inf. Proc. **15**, 3243 (2016).
- [62] M. Walter, D. Gross, and J. Eisert, *Multi-partite entanglement*, arXiv:1612.02437 [quant-ph].
- [63] A. Bera, S. Mal, A. Sen(De), and U. Sen, *Witnessing bipartite entanglement sequentially by multiple observers*, Phys. Rev. A **98**, 062304 (2018).
- [64] S. Roy, A. Bera, S. Mal, A. Sen(De), U. Sen, *Recycling the resource: Sequential usage of shared state in quantum teleportation with weak measurements*, arXiv:1905.04164 [quant-ph].